Rev-erbα and Rev-erbβ coordinately protect the circadian clock and normal metabolic function

Anne Bugge, Dan Feng, Logan J. Everett, Erika R. Briggs, Shannon E. Mullican, Fenfen Wang, Jennifer Jager, and Mitchell A. Lazar[1]

Division of Endocrinology, Diabetes, and Metabolism, Department of Medicine, Department of Genetics, The Institute for Diabetes, Obesity, and Metabolism, Perelman School of Medicine at the University of Pennsylvania, Philadelphia, Pennsylvania 19104, USA

The nuclear receptor Rev-erbα regulates circadian rhythm and metabolism, but its effects are modest and it has been considered to be a secondary regulator of the cell-autonomous clock. Here we report that depletion of Rev-erbα together with closely related Rev-erbβ has dramatic effects on the cell-autonomous clock as well as hepatic lipid metabolism. Mouse embryonic fibroblasts were rendered arrhythmic by depletion of both Rev-erbs. In mouse livers, Rev-erbβ mRNA and protein levels oscillate with a diurnal pattern similar to that of Rev-erbα, and both Rev-erbs are recruited to a remarkably similar set of binding sites across the genome, enriched near metabolic genes. Depletion of both Rev-erbs in liver synergistically derepresses several metabolic genes as well as genes that control the positive limb of the molecular clock. Moreover, deficiency of both Rev-erbs causes marked hepatic steatosis, in contrast to relatively subtle changes upon loss of either subtype alone. These findings establish the two Rev-erbs as major regulators of both clock function and metabolism, displaying a level of subtype collaboration that is unusual among nuclear receptors but common among core clock proteins, protecting the organism from major perturbations in circadian and metabolic physiology.

[*Keywords*: Rev-erb; nuclear receptors; circadian rhythm; metabolism]

Supplemental material is available for this article.

Received January 10, 2012; revised version accepted March 1, 2012.

Circadian rhythm is a fundamental regulatory factor in cells throughout the body of most organisms (Wijnen and Young 2006). It affects many aspects of behavior and physiology, including sleep/wake cycles, blood pressure, body temperature, and metabolism, and is thought to be an adaptation that provides the advantage of anticipating daily changes in the environment, rather than just responding (Takahashi et al. 2008). Disruption in circadian rhythm leads to increased incidence of many diseases, such as metabolic disorders, mental illness, and cancer (Gachon et al. 2004; Sahar and Sassone-Corsi 2009; Huang et al. 2011). The autonomous rhythm of the individual cell is entrained by hormonal and neuronal signals from a central clock located in the suprachiasmatic nuclei (SCN) of the hypothalamus, which is reset daily by light (Gachon et al. 2004; Sahar and Sassone-Corsi 2009; Huang et al. 2011). Some organs are not exclusively entrained to the environment by the SCN. For example, although hepatic glucose production (La Fleur 2003) and expression of several genes encoding lipogenic enzymes (Lanza-Jacoby et al. 1986) are circadian, the phase is tuned more directly to feeding activity (Gachon et al. 2004; Huang et al. 2011). The link between circadian rhythm and metabolic homeostasis is also evident from the observation that systemic perturbations in circadian rhythm result in hypoglycemia and altered insulin sensitivity (Rudic et al. 2004). Interestingly, shift work is linked to several metabolic disorders in humans (Esquirol et al. 2009).

Gene expression and the activity of gene products are coordinated in 24-h cycles throughout the body, with each cell having its own autonomous clock (Wijnen and Young 2006; Takahashi et al. 2008), but the biochemical mechanisms that maintain this coordination and the interplay with metabolic cues are not fully understood. The circadian cycle starts when two proteins—BMAL and CLOCK/NPAS2—heterodimerize to activate several clock genes, including *Per* and *Cry*. As a negative feedback loop, PER and CRY inhibit their own transcription by binding to BMAL and CLOCK/NPAS2. An important additional negative feedback loop requires the transcriptional repression function of the nuclear receptor (NR) Rev-erbα (NR1D1) (Lazar et al. 1989; Miyajima et al. 1989). Rev-erbα recruits

[1]**Corresponding author.**
E-mail lazar@mail.med.upenn.edu.
Article is online at http://www.genesdev.org/cgi/doi/10.1101/gad.186858.112.

the NR corepressor (NCoR)/histone deacetylase 3 (HDAC3) complex (Lazar 2003; Privalsky 2004) to repress transcription of *Bmal1* during the circadian night (Etchegaray et al. 2003; Yin and Lazar 2005). The *Rev-erbα* gene itself is activated by BMAL1 and CLOCK/NPAS2 and thereby represents an important link between the positive and negative loops of the circadian clock. Indeed, mice lacking Rev-erbα manifest disordered circadian rhythm (Preitner et al. 2002).

We showed previously that, in the mouse liver, the Rev-erbα cistrome consists of thousands of genomic binding sites with a circadian rhythm that follows the dramatically oscillating expression of Rev-erbα itself (Feng et al. 2011). The NCoR and HDAC3 cistromes are highly correlated with that of Rev-erbα (Feng et al. 2011; Sun et al. 2011) and exhibit a circadian rhythm even though NCoR and HDAC3 levels do not oscillate throughout the day (Feng et al. 2011). The Rev-erbα, NCoR, and HDAC3 cistromes are enriched for genes involved in lipid metabolism. Deletion of HDAC3 leads to dysregulation of hepatic lipid homeostasis, resulting in massive steatosis (Feng et al. 2011). Loss of Rev-erbα also leads to hepatosteatosis (Feng et al. 2011), but the effect is much more modest, suggesting that the more robust effect of HDAC3 depletion requires an additional factor.

A prime candidate is Rev-erbβ (NR1D2), whose DNA-binding domain (DBD) in mice is ~96% identical to that of Rev-erbα (CLUSTAL W) (Retnakaran et al. 1994) and has been shown to bind the canonical Rev-erbα-binding site (Dumas et al. 1994; Woo et al. 2007; Pardee et al. 2009). Interestingly, among the NRs, only the estrogen receptors (ERs) display the same degree of DBD conservation among the two subtypes (CLUSTAL W). Although their DBDs are nearly identical, the overall homology between the Rev-erb subtypes is only ~49%, mainly due to lack of conservation of the N-terminal A/B domains and the exceptionally long mid-molecule D domains (CLUSTAL W). The biology of Rev-erbβ has not been nearly as well described as that of Rev-erbα (Bonnelye et al. 1994; Dumas et al. 1994; Retnakaran et al. 1994). Rev-erbβ affects the amplitude of a *Bmal1*:luciferase reporter in mouse embryonic fibroblasts (MEFs) (Liu et al. 2008) and regulates expression of apolipoprotein C-III in hepatocytes (Wang et al. 2007, 2008) and genes involved in lipid absorption in skeletal muscle cells (Ramakrishnan et al. 2005), but little else is known about the function or regulation of Rev-erbβ in circadian rhythm and metabolism.

Here we demonstrate the physiological function of Rev-erbβ in the regulation of circadian rhythm and metabolism and the consequences of total hepatic Rev-erb deficiency. Remarkably, the cistromes of Rev-erbα and Rev-erbβ are nearly identical, and loss of both Rev-erbs in the liver leads to dramatic derepression of clock genes and marked hepatosteatosis. Thus, our data show that the activities of the two Rev-erb subtypes are coordinated to protect against major perturbations in circadian and metabolic physiology.

Results

Loss of both Rev-erb subtypes renders cells arrhythmic

Rev-erbβ was depleted in MEFs, derived from wild-type and Rev-erbα-null embryos, using an adenovirus expressing a shRNA targeting Rev-erbβ. Following serum shock to synchronize the cells, rhythmic expression of Rev-erbα mRNA was observed in wild-type MEFs depleted of Rev-erbβ (Fig. 1A), and conversely, rhythmic expression of Rev-erbβ mRNA was maintained in Rev-erbα-null MEFs (Fig. 1B). Similarly, and reminiscent of previous studies (Liu et al. 2008), we observed that deficiency of either Rev-erbα or Rev-erbβ did not abrogate the circadian expression of core clock gene *Bmal1* (Fig. 1C). In contrast, knockdown of Rev-erbβ in Rev-erbα-null MEFs led to a pronounced decrease in Bmal1 mRNA amplitude and progressive loss of rhythmic expression (Fig. 1D). Likewise, Cry1 mRNA displayed a robust rhythm when a single Rev-erb subtype was deficient (Fig. 1E), but this was markedly attenuated when MEFs were depleted of both Rev-erbs (Fig. 1F). These results demonstrated that normal rhythmic gene expression requires the presence of at least one Rev-erb subtype.

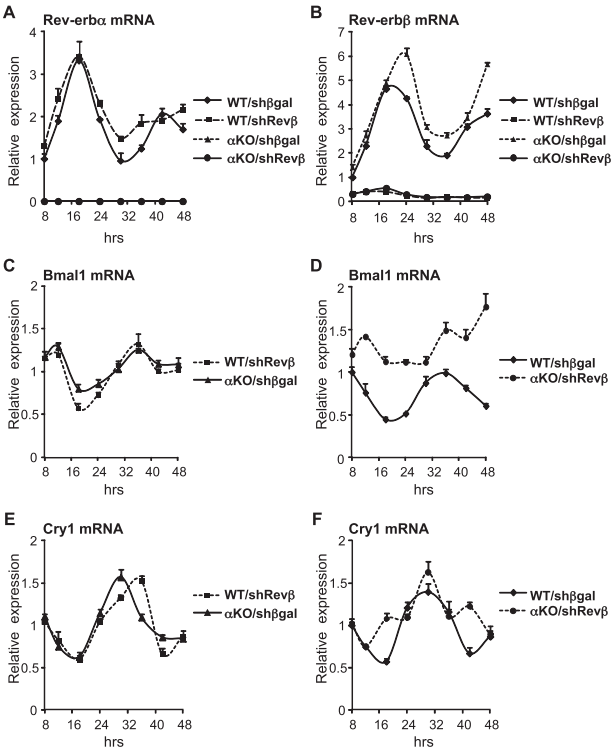

Figure 1. Loss of both Rev-erb subtypes renders MEFs arrhythmic. Gene expression over a 40-h period in synchronized wild-type (WT) or Rev-erbα knockout (αKO) MEFs transduced with adenovirus encoding a shRNA targeting Rev-erbβ (Revβ) or βgal as control. The experiment was performed in triplicate, and SEM is indicated by vertical bars. All values have been normalized to Arbp mRNA expression and the 8-h time point in the wild-type control. (*A*) Rev-erbα mRNA levels in wild-type MEFs infected with control virus (WT/shβgal) or Rev-erbβ knockdown virus (WT/shRevβ) and Rev-erbα-null MEFs infected with control virus (αKO/shβgal) or Rev-erbβ knockdown virus (αKO/shRevβ). (*B*) Rev-erbβ mRNA levels in the cells described in *A*. (*C*) Bmal1 mRNA levels in WT/shRevβ and αKO/shβgal cells. (*D*) Bmal1 mRNA levels in WT/shβgal and αKO/shRevβ cells. (*E*) Cry1 mRNA levels in WT/shRevβ and αKO/shβgal cells. (*F*) Cry1 mRNA levels in WT/shβgal and αKO/shRevβ cells.

Diurnal expression and genomic binding of Rev-erbβ in mouse livers

The collaboration of Rev-erbα and Rev-erbβ in the maintenance of rhythmic gene expression in MEFs prompted us to investigate the physiological role of Rev-erbβ and the consequences of complete hepatic Rev-erb deficiency in vivo. In agreement with previous studies (Panda et al. 2002), hepatic Rev-erbβ mRNA expression followed a diurnal rhythm comparable with that of Rev-erbα, with the peak occurring between 1:00 and 5:00 p.m. (Zeitgeber time 6–10 [ZT6–ZT10]) and the trough occurring between 5:00 and 9:00 a.m. (ZT22–ZT2) (Fig. 2A). As protein levels of endogenous Rev-erbβ have not previously been evaluated due to lack of a suitable antibody, we developed a polyclonal rabbit antiserum that specifically recognized Rev-erbβ (Supplemental Fig. 1). By immunoblot, this antibody revealed that Rev-erbβ protein levels followed a diurnal pattern that paralleled Rev-erbβ mRNA expression (Fig. 2B). Chromatin immunoprecipitation (ChIP) with this antibody, followed by site-specific PCR (ChIP-PCR), revealed Rev-erbβ binding to genomic Rev-erbα-binding sites with a diurnal profile (Fig. 2C) that was similar to that of Rev-erbα (Fig. 2D), with both Rev-erbs displaying strong binding at 5:00 p.m./ZT10 and weak binding at 5:00 a.m./ZT22.

The mouse liver Rev-erbβ cistrome is remarkably similar to that of Rev-erbα

We next used ChIP followed by deep sequencing (ChIP-seq) to determine the mouse liver Rev-erbβ cistrome at different times of day. Consistent with the expression of Rev-erbβ, many more binding regions were detected at 5:00 p.m. (19,782) than at 5:00 a.m. (1077; HOMER [Heinz et al. 2010], 0.1% false discover rate [FDR], ≥1 read per million [RPM]) (Fig. 3A). Interestingly, the 5:00 p.m. Rev-erbβ peak calls showed a 63% overlap with the previously reported 5:00 p.m. liver Rev-erbα cistrome (Feng et al. 2011). However, representative sites that appeared to be Rev-erbα-specific based on the ChIP-seq data persisted in Rev-erbα-null livers and could not be confirmed with a second Rev-erbα antibody (Supplemental Fig. 2), suggesting that these might be antibody-specific false positives, quite distinct from well-validated Rev-erbα sites such as in the *Bmal1* gene that are not observed in the Rev-erbα-null liver (Feng et al. 2011). To distinguish true binding events from these false positives genome-wide, ChIP-seq was performed on livers harvested from Rev-erbα-null mice at 5:00 p.m. using the same antibody that was used to generate the wild-type Rev-erbα cistrome (Feng et al. 2011), and these sites were filtered out in the subsequent analyses.

Furthermore, we realized that many of the regions that appeared to display Rev-erb subtype-specific binding based on peak calls actually had comparable ChIP-seq peak height signals for Rev-erbα and Rev-erbβ. Merging the peak calls identified in either the Rev-erbα and/or Rev-erbβ ChIP-seq experiments but not detected in the Rev-erbα-null mouse resulted in 31,958 regions, and quantitative analysis that directly compared the levels of ChIP-seq signals revealed that 92% (29,462) of these sites are bound by both subtypes and showed highly correlated ChIP-seq signals (r^2 = 0.78) (Fig. 3B). The best-fit line for these common sites is most likely skewed toward the Rev-erbα cistrome because of the slightly higher ChIP efficiency of this antibody. Indeed, the majority of peaks called as Rev-erbα-specific (5%) displayed some level of Rev-erbβ binding, suggesting that these sites should be regarded as regions bound preferentially by Rev-erbα, rather than true subtype-specific sites. For the 3% of sites with putative Rev-erbβ-specific binding, de novo motif analysis by HOMER did not identify any motif previously reported to be bound by the Rev-erbs; ~23% of these sites remained bound at both 5:00 p.m. and 5:00 a.m., and unlike bona fide sites, none of those tested were lost upon Rev-erbβ depletion (Supplemental Fig. 3), suggesting that there may be very few truly Rev-erbβ-specific binding sites. Thus, the cistromes of Rev-erbα and Rev-erbβ in the mouse liver are remarkably similar.

The shared Rev-erb cistrome constitutes a comprehensive list of high-confidence hepatic Rev-erb-binding sites, since

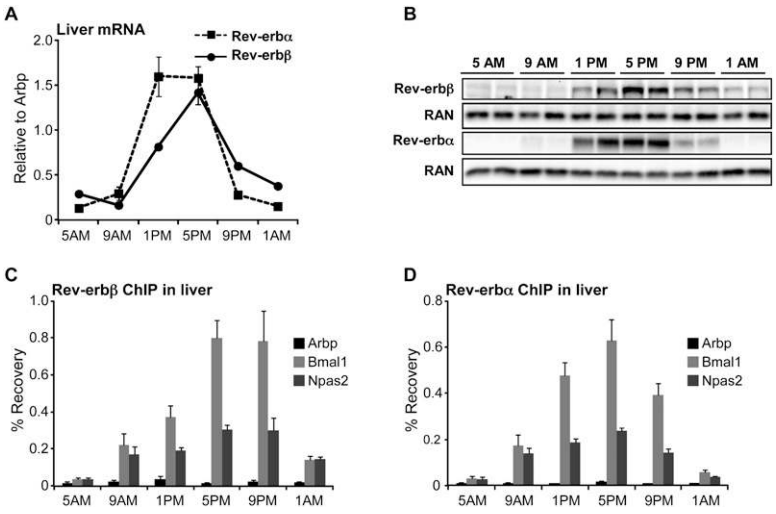

Figure 2. Diurnal rhythm of Rev-erbβ expression and genomic binding in mouse livers. (*A*) Rev-erb mRNA levels in the livers of 12-wk-old wild-type male mice euthanized at the indicated time points. n = 4 or 5; SEM is indicated by vertical bars. (*B*) Rev-erb protein levels. Western blot of liver extracts from 12-wk-old wild-type male mice euthanized at the indicated time points. The same extract was used on both blots. Ras-related nuclear protein (RAN) was used as a loading control. (*C*) Rev-erbβ ChIP on the liver samples described in *B*; *Arbp* intron 3 is a negative control region; n = 3 or 4; SEM is indicated by vertical bars. (*D*) Rev-erbα ChIP on the samples described in *B* and *C*. *Arbp* intron 3 is a negative control region; n = 3 or 4; SEM is indicated by vertical bars.

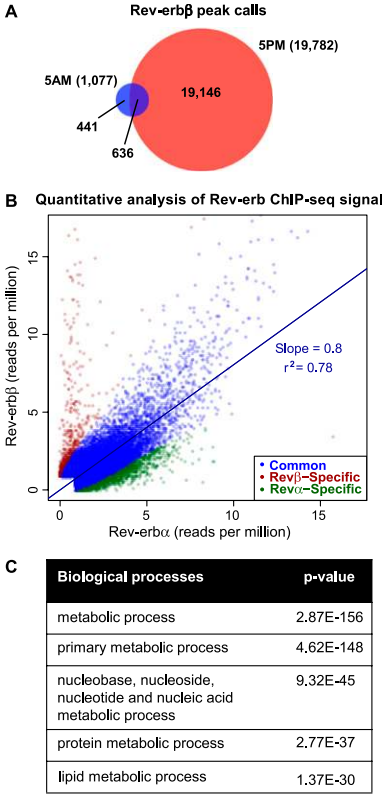

C

Biological processes	p-value
metabolic process	2.87E-156
primary metabolic process	4.62E-148
nucleobase, nucleoside, nucleotide and nucleic acid metabolic process	9.32E-45
protein metabolic process	2.77E-37
lipid metabolic process	1.37E-30

Figure 3. Extensive correlation of liver Rev-erbβ and Rev-erbα cistromes. (*A*) Overlap of the liver Rev-erbβ cistromes generated at 5:00 a.m. and 5:00 p.m. Binding sites were considered overlapping when the peak calls overlapped by at least 1 bp. Numbers indicate the total number of binding sites in each cistrome and the number of binding sites in each group. (*B*) Quantitative analysis of Rev-erb ChIP-seq signal. Scatter plot of the maximum stack height at each Rev-erbα and Rev-erbβ site not detected by Rev-erbα ChIP in the Rev-erbα-null mouse. Sites are classified as subtype-specific if the difference in binding profiles is statistically significant (Fisher's exact test, Benjamini-Hochberg-corrected *P*-value < 0.05) and indicates at least a two-fold difference in binding strength. For clarity, 16 common and 23 Rev-erbβ-specific outliers were omitted from the plot. r^2 and the slope of the best-fit line are shown for common sites. (*C*) Gene ontology analysis (PANTHER) on genes with a Rev-erb-binding site within 10 kb of the TSS (Galaxy/Cistrome). Shown are the top five enriched GO terms.

these same regions were identified with two independent Rev-erb subtype-specific antibodies. Ontology analysis (PANTHER) of genes with a Rev-erb-binding site within 10 kb of the transcription start site (TSS) revealed enrichment for metabolic processes, with lipid metabolism among the top three specialized pathways (Fig. 3C), in agreement with earlier analysis of the Rev-erbα cistrome only (Feng et al. 2011). Also, as previously noted for HDAC3 (Feng et al. 2011), Rev-erb binding is found primarily in proximity of active genes (Supplemental Fig. 4), consistent with the hypothesis that the Rev-erb/NCoR/HDAC3 complex functions to transiently modulate the activity of these active genes in a circadian manner.

Rev-erbα and Rev-erbβ bind simultaneously to nearby genomic sites

The binding of Rev-erbα and Rev-erbβ appeared to be centered at the same genomic positions, along with the NCoR/HDAC3 corepressor complex, as illustrated at the *Bmal1* gene (Fig. 4A). The most frequently identified motif at sites bound by both subtypes using de novo analysis was a variant of the classical NR AGGTCA half-site (HOMER, *P*-value = 1×10^{-701}). In addition, HOMER identified a half-site with an A/T-rich 5′ flank (*P*-value = 1×10^{-313}) (Fig. 4B), similar to the empirically determined Rev-erb-binding site (Harding and Lazar 1993), which is also referred to as an RORE motif (Giguère et al. 1994).

Recruitment of NCoR by Rev-erbα requires two monomers binding in close proximity (Harding and Lazar 1995; Yin and Lazar 2005). Sequential ChIP for Rev-erbα and Rev-erbβ revealed that both Rev-erbs were simultaneously present at binding sites in the promoters of *Bmal1* (Preitner et al. 2002; Yin and Lazar 2005) and *Npas2* (Crumbley et al. 2010) in the liver genome at 5:00 p.m. (Fig. 4C). However, there did not appear to be competition between the Rev-erb subtypes, as Rev-erbβ binding to these sites was unchanged in Rev-erbα-null mice (Supplemental Fig. 5). Previous work has shown that NCoR and HDAC3 are also bound at these sites (Feng et al. 2011), suggesting that Rev-erbα and Rev-erbβ can collaborate interchangeably in forming a functional transcriptional repression unit. From these data, we hypothesized that the shared Rev-erb cistrome would be enriched for close pairs or multiples of binding sites. Indeed, any given peak of Rev-erb binding was more likely to be located near a second peak than would be found randomly in the genome (Fig. 4D). The enrichment of proximal pairs of Rev-erb binding increased as the distance shortened, except below a distance of 200 base pairs (bp). However, we considered that the apparent falloff at 200 bp could be an artifact of the resolution of ChIP-seq, such that two or more sites might also appear in our data as a single peak call; indeed, the peak at the *Bmal1* gene is known to contain two Rev-erb half-sites (Preitner et al. 2002; Yin and Lazar 2005). To address this, the top de novo core motif identified for Rev-erb binding was used to scan the center of all of the peaks that comprise the common Rev-erb cistrome. Reassuringly, the NR half-site was found within the 100-bp center of ~65% of the Rev-erb peaks. Remarkably, the frequency of two or more sites under the peaks was 2.8-fold greater than random genomic regions (Fig. 4E). Thus, many of the peaks in the shared Rev-erb cistrome contain two or more half-sites, raising the possibility that Rev-erbα and/or Rev-erbβ could bind at adjacent sites within these regions.

Rev-erbβ protects clock and metabolic genes from the loss of Rev-erbα

The strong correlation between the binding of Rev-erbα and Rev-erbβ throughout the genome suggested that Rev-erbβ might repress many of the same genes as Rev-erbα. This was tested using adenovirus-expressing shRNA to deplete Rev-erbβ specifically in the liver of wild-type and Rev-erbα-null mice (Supplemental Fig. 6). In this manner, >80% depletion of Rev-erbβ mRNA (Fig. 5A), corresponding

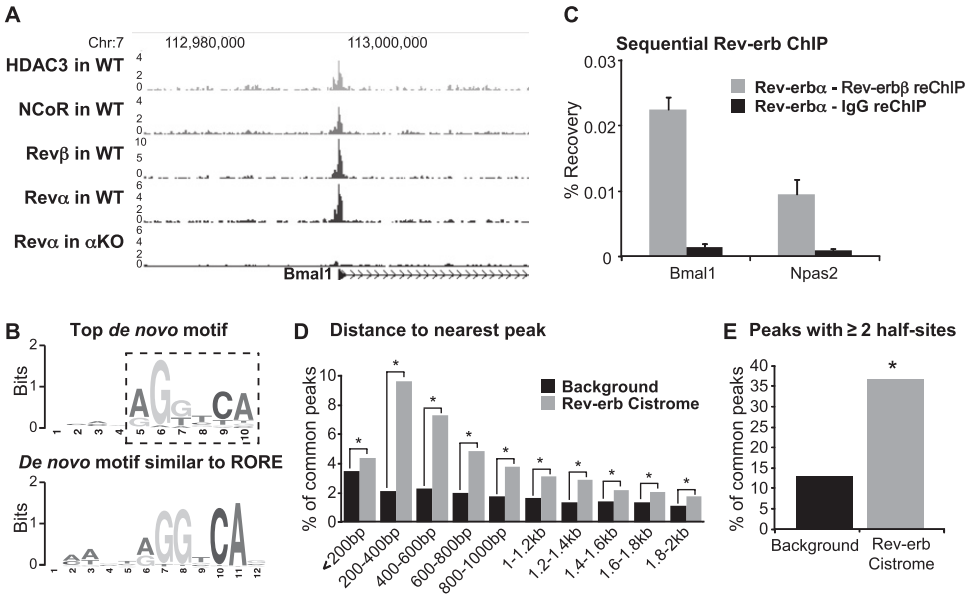

Figure 4. The Rev-erb subtypes bind simultaneously to genomic sites. (*A*) At 5:00 p.m., hepatic Rev-erbβ, Rev-erbα, NCoR, and HDAC3 bind together at two neighboring sites in the *Bmal1* promoter. Genome browser tracks of stack height profiles from ChIP-seq experiments for HDAC3 (Feng et al. 2011), NCoR (Feng et al. 2011), Rev-erbβ (Revβ), and Rev-erbα (Revα) in wild-type mice (Feng et al. 2011), and Rev-erbα in Rev-erbα knockout mice (αKO). Peak height is represented in reads per million. (*B*) Top de novo motif under the shared Rev-erb-binding sites (HOMER, *P*-value = 1×10^{-701}) with the core NR-binding motif boxed by a dashed outline, and the significantly enriched de novo motif similar to the published RORE (HOMER, *P*-value = 1×10^{-313}). (*C*) The Rev-erb subtypes are present simultaneously at the *Bmal1* and *Npas2* genes in the liver. Sequential ChIP of Rev-erbα followed by either Rev-erbβ or IgG ChIP in mouse livers harvested at 5:00 p.m. $n = 4$; SEM is indicated by vertical bars. (*D*) The distance to the nearest adjacent region was computed for each binding region in the common Rev-erb cistrome or randomly matched control sites and grouped in bins of 200 bp. (*) *P*-value < 1×10^{-7} (Fisher's exact test). (*E*) Identification of two or more binding motifs under Rev-erb peaks. All regions in the common Rev-erb cistrome were scanned for the core NR motif identified by de novo motif analysis (dashed outline; Fig. 3B) and compared with randomly selected control regions with a similar distribution of distances from the nearest gene TSS. (*) *P*-value < 1×10^{-16} (Fisher's exact test).

to a similar decrease in protein level (Fig. 5B), was achieved. Rev-erbα mRNA and protein levels were unchanged by this manipulation (Fig. 5A,B).

Rev-erbβ knockdown in the liver of wild-type mice led to derepression of *Bmal1* as well as several other genes involved in circadian rhythm and metabolism (Fig. 5C). The effect of Rev-erbβ knockdown was generally less than that of Rev-erbα deletion, particularly for clock genes, which could be due to residual Rev-erbβ or a dominant effect of Rev-erbα. Importantly, however, the loss of Rev-erbβ in the Rev-erbα-null background led to a further derepression of target genes at 5:00 p.m. (Fig. 5C), which was dramatic for the critical positive clock components *Bmal1* and *Npas2*.

Consistent with earlier studies of genes regulated by Rev-erbα (Duez et al. 2008; Le Martelot et al. 2009), we observed dysregulation of the bile metabolism gene *Cyp7a1* and its putative repressor, *E4bp4* (Supplemental Fig. 7A), although fecal bile acid and triglyceride excretion rates did not differ between wild-type mice and Rev-erbα-null mice with hepatic depletion of Rev-erbβ (Supplemental Fig. 7B). Interestingly, following a 12-h fast, mice with hepatic Rev-erb deficiency exhibited mild hypoglycemia and a significant increase in free fatty acids, with little change in serum triglycerides and ketones (Supplemental Fig. 8), similar to the fasting phenotype of mice lacking hepatic HDAC3 (Sun et al. 2012).

Complete Rev-erb deficiency disrupts the normal diurnal recruitment of NCoR and HDAC3 to the liver genome

We showed previously that the NCoR, HDAC3, and Rev-erbα cistromes are highly correlated in space and time and that deletion of Rev-erbα diminished recruitment of NCoR and HDAC3 to the liver genome at 5:00 p.m. (Feng et al. 2011). To address whether the mechanism underlying the additional derepression of Rev-erb target genes observed in the double Rev-erb-deficient animals could be explained by a further decrease in NCoR and HDAC3 recruitment, we performed ChIP-PCR for these factors in the livers of wild-type and Rev-erbα-null mice with and without Rev-erbβ depletion. Indeed, compared with the enrichment found in animals depleted of only one Rev-erb subtype, recruitment of both NCoR (Fig. 6A) and HDAC3 (Fig. 6B) was further decreased by complete Rev-erb deficiency at the binding regions near *Bmal1* and *Npas2*.

Rev-erbβ protects the liver from metabolic distress upon the loss of Rev-erbα

The coregulation of a common set of target genes by Rev-erbα and Rev-erbβ provided a potential explanation for the more pronounced hepatosteatosis caused by loss of HDAC3 than was observed in the Rev-erbα knockout mouse (Feng et al. 2011). One week of Rev-erbβ depletion

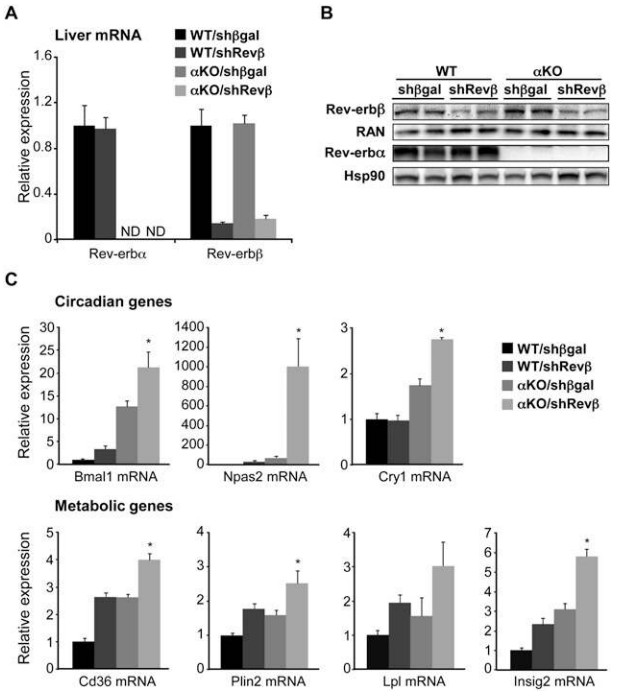

Figure 5. Rev-erbβ protects the regulation of clock and metabolic genes from loss of Rev-erbα. (*A*) shRNA-mediated knockdown of Rev-erbβ. Hepatic Rev-erb mRNA levels at 5:00 p.m., 7 d after tail vein injection of adenovirus encoding a shRNA targeting Rev-erbβ (Revβ) or βgal as control in 12-wk-old wild-type or Rev-erbα knockout (αKO) male mice. $n = 4–6$; SEM is indicated by vertical bars. (*B*) Western blots showing the Rev-erb protein levels in the livers of the mice described in *A*. The same extracts were loaded twice on separate gels and probed for either Rev-erbβ or Rev-erbα with Ras-related nuclear protein (RAN) or heat-shock protein 90 (Hsp90) as loading control, respectively. (*C*) Hepatic mRNA levels of circadian and metabolic genes in the mice described in *A*. (*) *P*-value ≤ 0.05 versus the αKO/shβgal condition as determined by Student's *t*-test.

did not have a significant effect on liver triglyceride levels, whereas chronic lack of Rev-erbα led to modest hepatosteatosis (Fig. 7). However, when Rev-erbβ levels were reduced in the Rev-erbα-null mouse, hepatosteatosis was markedly increased, with a large increase in triglyceride (Fig. 7A) as well as in Oil Red O staining for neutral lipids (Fig. 7B). Thus, Rev-erbα and Rev-erbβ collaborate in the regulation of hepatic lipid metabolism.

Discussion

We demonstrated that Rev-erbβ collaborates extensively with the closely related Rev-erbα subtype. In MEFs, both subtypes must be depleted to render *Bmal1* and *Cry1* expression arrhythmic, and in liver, both Rev-erbs display comparable diurnal patterns of gene and protein expression as well as correlated binding throughout the mouse genome. In contrast to the mild phenotype of the Rev-erbα-null mouse, dramatic effects on lipid and circadian physiological processes are observed when both Rev-erbs are lost. Thus, the similar expression and genomic binding of the two Rev-erbs serve to protect the circadian clock and normal metabolic function. Importantly, in addition to serving as a link between the circadian clock and metabolism, our findings suggest that Rev-erbα and Rev-erbβ are central components of the mammalian core clock (Fig. 8).

We and others (Sullivan et al. 2011) have observed that ChIP-seq experiments frequently contain a subset of nonspecific interactions and artifacts. In our efforts to continuously improve and obtain the highest quality of data in order to accurately describe Rev-erb biology, we filtered our Rev-erbα liver cistrome (Feng et al. 2011) by subtracting binding events that were also detected in the livers of Rev-erbα-null animals. When possible, performance of ChIP-seq on knockout samples should be considered as a standard control in genome-wide studies of transcription factor binding.

The cistromes of Rev-erbα and the NCoR/HDAC3 corepressor complex display significant spatial and circadian overlap in the liver (Feng et al. 2011). The demonstration of extensive correlation with Rev-erbβ binding at these sites provides a molecular basis for the observation that the fatty liver phenotype of mice lacking hepatic HDAC3 is more pronounced than that of Rev-erbα-null mice (Feng et al. 2011), as the modestly elevated hepatic triglyceride content of Rev-erbα-null mice increases dramatically upon depletion of Rev-erbβ. It should be noted that the hepatosteatosis of mice lacking hepatic HDAC3 is greater than in mice lacking both Rev-erbs, as described here; this could be due to the residual Rev-erbβ expression in the knockdown, a role for other transcription factors in HDAC3 function, and nonhistone targets of HDAC3.

Our discovery of extensive collaboration between the Rev-erb subtypes was surprising because subtype specificity is a recurring theme among NRs (Gauthier et al. 1999; Nielsen et al. 2006; Kang et al. 2007; Korach-André et al. 2010). Much of this subtype specificity can be ascribed to tissue-specific expression (Kuiper et al. 1997; Escher et al. 2001; Kang et al. 2007) and/or binding site selectivity (Nielsen et al. 2006). However, both Rev-erbs are expressed in major metabolic tissues, including fat, heart, and muscle

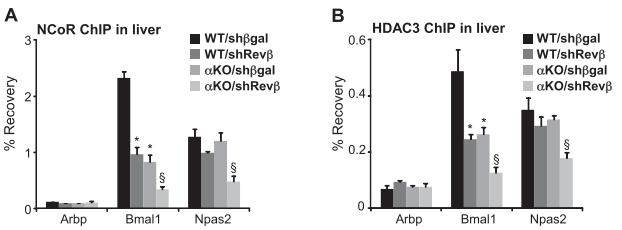

Figure 6. Complete Rev-erb deficiency disrupts NCoR and HDAC3 recruitment at 5:00 p.m. (*A*) NCoR ChIP in liver at 5:00 p.m., 7 d after tail vein injection of adenovirus encoding a shRNA targeting Rev-erbβ (Revβ) or βgal as control in 12-wk-old wild-type or Rev-erbα-null (αKO) male mice. *Arbp* intron 3 is a negative control region; $n = 3$; SEM is indicated by vertical bars. (*) *P*-value ≤ 0.05 relative to WT/shβgal; (§) *P*-value ≤ 0.05 relative to all other treatments, as determined by a Student's *t*-test. (*B*) HDAC3 ChIP on liver extracts from the mice described in *A*. *Arbp* intron 3 is a negative control region; $n = 3$; SEM is indicated by vertical bars. (*) *P*-value ≤ 0.05 relative to WT/shβgal; (§) *P*-value ≤ 0.05 versus all other treatments, as determined by Student's *t*-test.

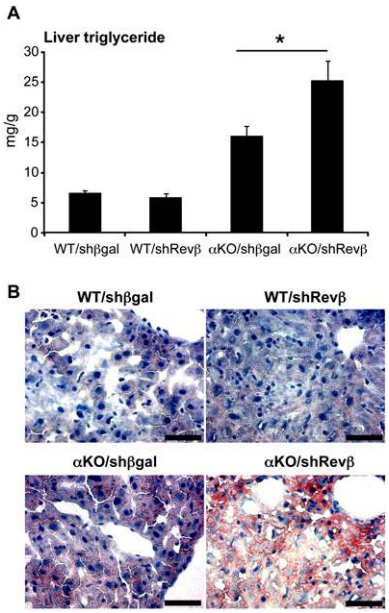

Figure 7. Total hepatic Rev-erb deficiency leads to exacerbated steatosis. (*A*) Hepatic triglyceride levels in two pooled experiments of 12-wk-old wild-type or Rev-erbα knockout (αKO) mice 7 d after injection of adenovirus encoding shRNA targeting Rev-erbβ (Revβ) or βgal as control. n = 5–7; SEM is indicated by vertical bars. (*) P-value = 0.0272 as determined by Student's t-test. (*B*) Oil red O stains of liver sections from the mice described in *A* at a magnification of 40× Bar, 50 μm.

in addition to liver (A Bugge, unpubl.; http://www.nursa.org/10.1621/datasets.02001). Moreover, the Rev-erb DBDs are 96% identical, which is matched only by ERα and ERβ, which tend to be expressed in different cell types (Kuiper et al. 1997). The near identity of the Rev-erbα and Rev-erbβ cistromes is even more remarkable considering that a single factor, such as ERα, may have quite different cistromes in the same cell type due to different activating signals (Lupien et al. 2010).

Thus, it appears that the coordinated activities of Rev-erbα and Rev-erbβ are required for normal liver clock gene expression and lipid metabolism. Intriguingly, the core clock proteins CLOCK, CRY, and PER all have homologs that serve a backup function, and although the BMAL1-null mouse is highly arrhythmic, it has been reported that BMAL2 expression is abolished by BMAL1 ablation, but overexpression of BMAL2 can compensate for loss of BMAL1 (Shi et al. 2010). Accordingly, for all clock components, loss of only one homolog has relatively minor effects, while depletion of all subtypes causes severe circadian phenotypes (van der Horst et al. 1999; Bae et al. 2001; DeBruyne et al. 2007; Shi et al. 2010), similar to what we found for the Rev-erbs. Taken together, our data thus suggest that the relationship between Rev-erbα and Rev-erbβ is more reminiscent of that of core clock proteins, where a backup system exists for every component, in contrast to most other NR subtype families.

Rev-erbα is known to self-regulate by feedback inhibition (Adelmant et al. 1996), and we observed binding of both Rev-erbs at the *Rev-erbα* gene. However, neither Rev-erb was bound in proximity to *Rev-erbβ*, suggesting that although both genes are expressed with a circadian pattern and are regulated post-transcriptionally by binding to heme (Raghuram et al. 2007; Yin et al. 2007), they may be regulated differently under some circumstances. This likely applies to post-translational regulation as well, since an N-terminal GSK3β site that is conserved in Rev-erbα of different species and controls its interaction with E3 ligases and proteasomal degradation (Yin et al. 2006, 2010) is absent in Rev-erbβ. Thus, the two Rev-erbs are less prone to concomitant dysregulation, further protecting the clock and metabolic pathways from selected perturbations.

The extensive collaboration of the Rev-erb subtypes implies that these NRs play a more critical role at the intersection of circadian regulation and metabolism than previously appreciated. Our findings thus highlight the importance of the intricate interplay between circadian rhythm and metabolism in maintaining lipid homeostasis and organismal health. This key role of the Rev-erbs and the ability to manipulate their activities by pharmacological ligands (Grant et al. 2010; Kumar et al. 2010; Kojetin et al. 2011) suggest that treatments for circadian and/or metabolic disorders may need to alter the activity or stability of both Rev-erbα and Rev-erbβ.

Materials and methods

Animals

Wild-type C57Bl/6 mice were purchased from Jackson Laboratories. The Rev-erbα knockout mice were obtained from B. Vennström, and backcrossed seven or more generations with C57Bl/6 mice. Eight-week-old to 12-wk-old wild-type and mutant male mice were housed under 12-h-light/12-h-dark cycles (lights on at 7:00 a.m., lights off at 7:00 p.m.) and euthanized at ZT10 (5:00 p.m.) or ZT22 (5:00 a.m.). The 12-h fast was conducted from 5:00 a.m. to 5:00 p.m. All of the animal care and use procedures followed the guidelines of the Institutional Animal Care and Use Committee of the University of Pennsylvania.

Antibodies

The HDAC3 antibody was purchased from Abcam (ab7030), Rev-erbα antibody was purchased from Cell Signaling Technology (#2124) and Santa Cruz Biotechnology (sc-47625), Ran antibody was purchased from BD Transduction Laboratories (#610341), Hsp90 antibody was purchased from Santa Cruz Biotechnology (sc-33755), normal rabbit IgG was purchased from Santa Cruz Biotechnology (sc-2027), Flag antibody was purchased from Sigma-Aldrich (F1804), and the NCoR antibody has previously been described (Huang et al. 2000; Feng et al. 2011). The Rev-erbβ antibody was raised in a rabbit against amino acids 243–261 (Covance).

Constructs and gene transductions

Rev-erbα and Rev-erbβ were Flag-tagged by cloning into the p3XFlag-CMV-7.1 vector (Sigma-Aldrich) and transfected into 293T cells using Lipofectamine (Invitrogen). The adenoviruses encoding shRNA targeting the β-galactosidase (TGCACCTGG TAAATCTTAT) or the Rev-erbβ gene (GCACTAAGGACCTTA ATAATG) were constructed using the BLOCK-iT adenoviral RNAi

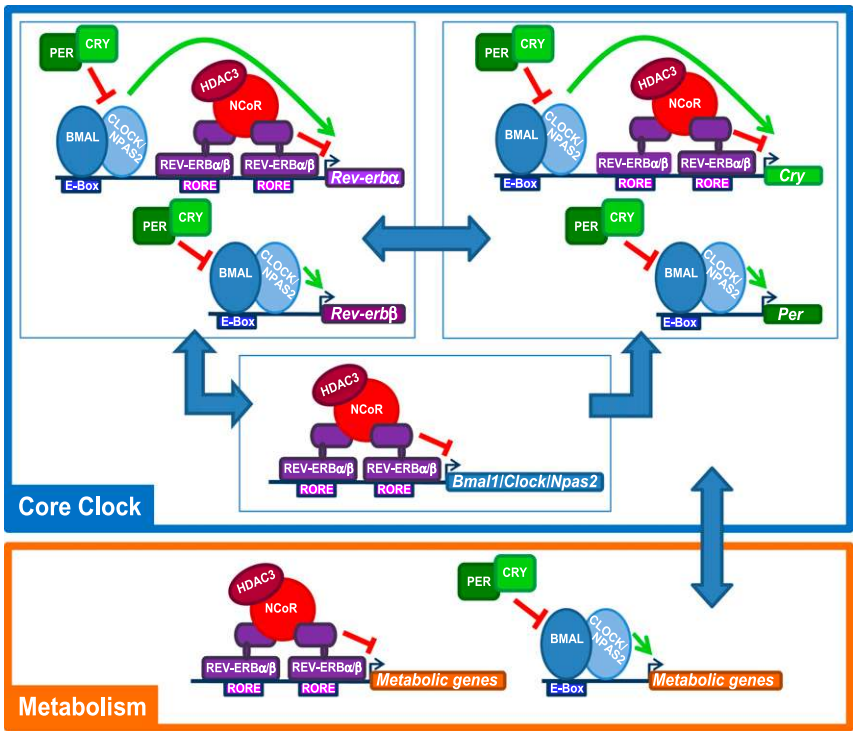

Figure 8. Rev-erbα and Rev-erbβ cooperate in regulating core clock function and mediating the interplay between circadian rhythm and metabolism. The Rev-erbs are central repressors of both the positive (*Bmal1*) and the negative (*Cry1* and *Rev-erbα*) limb of the core clock. In addition, the Rev-erbs mediate the interplay between the cellular clock and metabolism together with BMAL1 and CLOCK/NPAS2. Note that other core clock components (shown as PER, CRY, and BMAL in the model for simplicity) all have homologs (PER1–3, CRY1/2, and BMAL1/2) that, like the two Rev-erb subtypes, function as a backup system.

expression system from Invitrogen (#K4941-00) and subsequently amplified and purified by the Vector Core of the Penn Diabetes Research Center. Each mouse received 5.7×10^{11} particles (GC) of virus through tail vein injection.

Immunoprecipitation

Cells were washed with PBS, harvested in immunoprecipitation lysis buffer (50 mM Tris-HCl, 150 mM NaCl, 1% NP-40 at pH 8), and incubated for 30 min on ice, followed by sonication in the Bioruptor (Diagenode) for 3×20 sec at the lowest intensity. After centrifugation at 10.000*g* for 15 min, the extracts were divided into two and subjected to immunoprecipitation overnight with Rev-erbβ antibody or normal rabbit IgG. The immunoprecipitated proteins were eluted by boiling in SDS sample buffer and analyzed by SDS-PAGE.

Synchronized MEFs

MEFs were collected at embryonic day 13.5 from wild-type or Rev-erbα-null embryos, expanded, and seeded in 24-well plates at a density of 5×10^4 cells per well. The MEFs were washed in PBS and incubated for 20 h with 5.7×10^9 particles (GC) of adenovirus per well in DMEM containing 0.5% bovine serum. Serum shock was performed by replacing starvation medium with 50% horse serum for 2 h. Following two washes in PBS, cells were changed back to DMEM containing 0.5% bovine serum, and total RNA was harvested at the indicated time points.

ChIP

Mouse liver was harvested immediately after euthanasia. It was quickly minced and cross-linked in 1% formaldehyde for 20 min, followed by quenching with 1/20 vol of 2.5 M glycine solution and two washes with 1× PBS. Nuclear extracts were prepared by Dounce homogenization in cell lysis buffer (5 mM PIPES, 85 mM KCl, 0.5% Igepal, and Complete protease inhibitor tablet from Roche at pH 8.0). Chromatin fragmentation was performed by sonication in ChIP SDS lysis buffer (50 mM HEPES, 1% SDS, 10 mM EDTA at pH 7.5) using the Bioruptor (Diagenode). Proteins were immunoprecipitated in ChIP dilution buffer (50 mM HEPES, 155 mM NaCl, 1.1% Triton X-100, 0.11% Na-deoxycholate, Complete protease inhibitor tablet at pH 7.5). Cross-linking was reversed overnight at 65°C in elution buffer (50 mM Tris-HCL, 10 mM EDTA, 1% SDS at pH 8), and DNA was isolated using phenol/chloroform/isoamyl alcohol. Precipitated DNA was analyzed by quantitative PCR. Re-ChIP was performed in essentially the same way, except that the first elution was carried out in a reducing elution buffer (1% SDS, 10 mM DTT), shaking at 800 rpm for 30 min at 37°C. The Rev-erbα ChIP eluate was then diluted 66× in ChIP dilution buffer, divided into two, and subjected to either Rev-erbβ or IgG ChIP.

Quantitative PCR

Quantitative PCR was performed with Power SYBR Green PCR Master Mix on the PRISM 7500 (Applied Biosystems) with the relative amount of amplicon generated and primer efficacy evaluatd by a standard curve in each run. Primer sequences can be found in Supplemental Table 1.

ChIP-seq

ChIP experiments were performed independently on liver samples from four different mice harvested at 5:00 a.m. or 5:00 p.m. ChIP of Rev-erbα in Rev-erbα-null mice was performed using the Cell Signaling Technology antibody (#2124). The precipitated DNA was subsequently pooled and amplified according to the ChIP Sequencing Sample Preparation Guide provided by Illumina using adaptor oligos and primers from Illumina, enzymes from New England Biolabs, and the PCR purification kit (#28104) and MinElute kit (#28004) from Qiagen. Deep sequencing was

performed by the Functional Genomics Core (J. Schug and K. Kaestner) of the Penn Diabetes Research Center using the Illumina Genome Analyzer IIx and Illumina HiSeq 2000, and sequences were obtained using the Solexa Analysis Pipeline. All data are available in Gene Expression Omnibus (GEO) under accession number GSE36375, and all previously published data (Feng et al. 2011) are available under accession number GSE26345.

ChIP-seq peak calling and data normalization

For all ChIP-seq samples, sequence reads were mapped to the mouse genome (NCBI36/UCSC mm8) using ELAND software. Only the sequences uniquely mapped with no more than two mismatches in the first 32 bp were kept and used as valid reads. Redundant reads mapping to the same genomic loci were condensed to a single read to remove clonal amplification artifacts. Reads from replicate samples were pooled together prior to further analysis. Peak calling was carried out by HOMER (version 3; 0.1% FDR, 1 RPM cutoff) (Heinz et al. 2010) on each ChIP-seq sample. To adjust for the higher read depth in the Rev-erbα-null ChIP-seq sample, reads were randomly sampled from the Rev-erbα-null data 10 times, such that each random sample had a read count similar to the wild-type cistrome. The peak height was computed in each random sample, and the average height at each peak was used for subsequent analysis. In order to obtain the most stringent high-confidence cistrome, potential nonspecific binding events in the Rev-erbα 5:00 p.m./ZT10 cistrome were identified, thereby removing 5830 peaks where the Rev-erbα ChIP-seq profile in the Rev-erbα-null animal was >50% of the peak height observed in the wild-type at 5:00 p.m./ZT10 from all subsequent analysis. The remaining peak calls for both Rev-erbα and Rev-erbβ were then merged together, such that any overlapping regions were combined into one region covering the peak calls for both isoforms. This resulted in 31,958 total Rev-erb-binding regions, which contain a valid peak call for Rev-erbα and/or Rev-erbβ. The ChIP-seq signal for each subtype was then quantified at each region by computing the maximum stack height profile within the region, normalized to the total number of reads for that subtype (RPM). Thus, for each Rev-erb-binding region, a pair of two values was computed: one representing the relative strength of binding by Rev-erbα, and the other representing the strength of binding by Rev-erbβ. For each binding region, these values were plotted on a scatter plot showing Rev-erbα on the *X*-axis and Rev-erbβ-binding strength on the *Y*-axis.

Each region was categorized as being specific to either subtype or common to both subtypes as follows: First, a Fisher's exact test was applied to each region, comparing the peak height and total reads for each factor for significant changes that are unlikely to occur simply due to variability in the sequencing process. Regions with a Benjamini-Hochberg-corrected *P*-value <0.05 from the Fisher's exact test and an absolute fold change >2 using the normalized (RPM) peak heights were considered to be specific to the subtype with greater binding. All other sites were considered "common" sites because, regardless of peak calls, these sites did not show a significant quantitative difference in binding signal between the two subtypes. By this method, 29,462 sites are considered "common" sites (92%), 1614 are considered "Rev-erbα-specific" (5%), and 882 are considered "Rev-erbβ-specific" (3%). Correlation and the best-fit line were computed from the "common" set of sites.

Cistromic analysis

A random set of matched controls with similar distances to the nearest TSS was generated for the 1614 Rev-erbα-specific, 882 Rev-erbβ-specific, and 29,462 common Rev-erb sites using CisGenome (Ji et al. 2008). Then, de novo motif analysis with HOMER (Heinz et al. 2010) was performed using 100 bp of sequence under each peak center and using the matched controls as background with masking of all repeat elements. For the top de novo motif in the common Rev-erb cistrome (NR half-site), the nonspecific positions around the core motif were removed, and the match score threshold was adjusted to account for shortening the motif. The number of nonoverlapping core NR motif matches under the same peak was then counted. Repeat of this analysis without masking of repeat elements led to similar results (data not shown). To test for proximal pairs of peaks, the distance to the nearest neighboring binding region was computed for both the common Rev-erb sites and matched controls. Subsets of active and inactive genes were defined using the same data and criteria as previously published (GSE25937) (Feng et al. 2011) and were used to compute the percentage of genes in each group with at least one common Rev-erb site within 10 kb of the TSS. For each expression group, the significance of the enrichment of Rev-erb binding relative to all genes on the array was tested using a Fisher's exact test.

Gene expression analysis

Total RNA was extracted from liver samples harvested from 12-wk-old male wild-type or Rev-erbα knockout mice 7 d after injection of shβgal or shRev-erbβ adenovirus using the RNeasy minikit (Qiagen). The RNA was reverse-transcribed using the High-Capacity cDNA Reverse Transcription kit (Applied Biosystems) and analyzed by quantitative PCR. Gene expression was normalized to the mRNA levels of the housekeeping gene *Arbp* and the level of the gene of interest in the control samples.

Immunoblotting

Liver samples were crushed and sonicated (5 min 30 sec on/off) in cold extraction buffer (25 mM Tris-HCl, 2 mM EDTA, 0.1% SDS, 150 mM NaCl, 50 mM KCl, 1% Triton X-100, 0.08% DOC at pH 8) supplemented with Complete protease inhibitors (Roche). SDS-PAGE was performed using 100 μg of protein loaded onto a 10% Tris-glycine gel (Invitrogen), followed by transfer to a PVDF membrane (Invitrogen). After incubation with antibodies, blots were developed using the enhanced chemiluminescence kit from PerkinElmer.

Hepatic triglyceride assay

Liver samples were homogenized using the TissueLyser (Qiagen) in tissue lysis buffer (140 mM NaCl, 50 mM Tris, 1% Triton-X at pH 8.0). Triglyceride concentration in the lysates was quantified using LiquiColor triglyceride procedure no. 2100 (Stanbio).

Oil Red O staining

Frozen sections (5 μM) were prepared from snap-frozen liver tissues and fixed in 10% buffered formalin for 3 min. The sections were then stained in 0.5% Oil Red O in propylene glycerol overnight for lipid and then in hematoxylin for nuclei for 5 sec.

Serum biochemistry

Blood glucose was measured using a OneTouch glucometer (Medtronic) on blood collected from the tail prior to euthanasia. Subsequently, blood was collected from the heart and left to clot for 30 min at room temperature, followed by centrifugation to isolate the serum. Triglycerides were quantified using LiquiColor triglyceride procedure no. 2100 (Stanbio), ketones were quantified using LiquiColor β-hydroxybutyrate procedure no. 2440 (Stanbio),

and free fatty acids were quantified using the HR series NEFA-HR(2) kit (Wako Diagnostics).

Fecal analysis

The mice were housed separately, and feces were collected, dried, and weighed over a 60-h period starting at 5:00 p.m. on day 4 post-injection of adenovirus. The bile acid excretion rate was determined as previously described (Yu et al. 2000). Briefly, bile acids were extracted from 0.5 g of minced feces in 75% EtOH for 2 h at 50°C. The extracts were diluted 1:3 in 25% PBS and analyzed using the Total Bile Acid assay from Diazyme. Fecal triglyceride content was determined essentially as previously described (Wong et al. 2007). Briefly, triglycerides were extracted from 50 mg of dry feces in EtOH:30% KOH (2:1) overnight at 60°C. One fold of 1 M $MgCl_2$ was added to the supernatant, followed by 10 min of incubation on ice and 30 min of centrifugation at 14,000 rpm. The triglyceride concentration of the extract was determined using LiquiColor triglyceride procedure no. 2100 (Stanbio).

Acknowledgments

We gratefully acknowledge the assistance of the Functional Genomics Core and Viral Vector Core of the Penn Diabetes Research Center (P30 DK19525), and the Morphology Core supported by P01 DK49210. This work was supported by NIH grant R01 DK45586 to M.A.L., the Cox Institute for Medical Research, and grants from the Danish Council for Independent Research (FNU) and the Lundbeck Foundation to A.B.

References

Adelmant G, Bègue A, Stéhelin D, Laudet V. 1996. A functional Rev-erbα responsive element located in the human Rev-erbα promoter mediates a repressing activity. *Proc Natl Acad Sci* **93:** 3553–3558.

Bae K, Jin X, Maywood ES, Hastings MH, Reppert SM, Weaver DR. 2001. Differential functions of mPer1, mPer2, and mPer3 in the SCN circadian clock. *Neuron* **30:** 525–536.

Bonnelye E, Vanacker JM, Desbiens X, Begue A, Stehelin D, Laudet V. 1994. Rev-erbβ, a new member of the nuclear receptor superfamily, is expressed in the nervous system during chicken development. *Cell Growth Differ* **5:** 1357–1365.

Crumbley C, Wang Y, Kojetin DJ, Burris TP. 2010. Characterization of the core mammalian clock component, NPAS2, as a REV-ERBα/RORα target gene. *J Biol Chem* **285:** 35386–35392.

DeBruyne JP, Weaver DR, Reppert SM. 2007. CLOCK and NPAS2 have overlapping roles in the suprachiasmatic circadian clock. *Nat Neurosci* **10:** 543–545.

Duez H, van der Veen JN, Duhem C, Pourcet B, Touvier T, Fontaine C, Derudas B, Baugé E, Havinga R, Bloks VW, et al. 2008. Regulation of bile acid synthesis by the nuclear receptor Rev-erbα. *Gastroenterology* **135:** 689–698.

Dumas B, Harding HP, Choi HS, Lehmann KA, Chung M, Lazar MA, Moore DD. 1994. A new orphan member of the nuclear hormone receptor superfamily closely related to Rev-Erb. *Mol Endocrinol* **8:** 996–1005.

Escher P, Braissant O, Basu-Modak S, Michalik L, Wahli W, Desvergne B. 2001. Rat PPARs: Quantitative analysis in adult rat tissues and regulation in fasting and refeeding. *Endocrinology* **142:** 4195–4202.

Esquirol Y, Bongard V, Mabile L, Jonnier B, Soulat JM, Perret B. 2009. Shift work and metabolic syndrome: Respective impacts of job strain, physical activity, and dietary rhythms. *Chronobiol Int* **26:** 544–559.

Etchegaray JP, Lee C, Wade PA, Reppert SM. 2003. Rhythmic histone acetylation underlies transcription in the mammalian circadian clock. *Nature* **421:** 177–182.

Feng D, Liu T, Sun Z, Bugge A, Mullican SE, Alenghat T, Liu XS, Lazar MA. 2011. A circadian rhythm orchestrated by histone deacetylase 3 controls hepatic lipid metabolism. *Science* **331:** 1315–1319.

Gachon F, Nagoshi E, Brown SA, Ripperger J, Schibler U. 2004. The mammalian circadian timing system: From gene expression to physiology. *Chromosoma* **113:** 103–112.

Gauthier K, Chassande O, Plateroti M, Roux JP, Legrand C, Pain B, Rousset B, Weiss R, Trouillas J, Samarut J. 1999. Different functions for the thyroid hormone receptors TRα and TRβ in the control of thyroid hormone production and post-natal development. *EMBO J* **18:** 623–631.

Giguère V, Tini M, Flock G, Ong E, Evans RM, Otulakowski G. 1994. Isoform-specific amino-terminal domains dictate DNA-binding properties of RORα, a novel family of orphan hormone nuclear receptors. *Genes Dev* **8:** 538–553.

Grant D, Yin L, Collins JL, Parks DJ, Orband-Miller LA, Wisely GB, Joshi S, Lazar MA, Willson TM, Zuercher WJ. 2010. GSK4112, a small molecule chemical probe for the cell biology of the nuclear heme receptor Rev-erbα. *ACS Chem Biol* **5:** 925–932.

Harding HP, Lazar MA. 1993. The orphan receptor Rev-ErbAα activates transcription via a novel response element. *Mol Cell Biol* **13:** 3113–3121.

Harding HP, Lazar MA. 1995. The monomer-binding orphan receptor Rev-Erb represses transcription as a dimer on a novel direct repeat. *Mol Cell Biol* **15:** 4791–4802.

Heinz S, Benner C, Spann N, Bertolino E, Lin YC, Laslo P, Cheng JX, Murre C, Singh H, Glass CK. 2010. Simple combinations of lineage-determining transcription factors prime *cis*-regulatory elements required for macrophage and B cell identities. *Mol Cell* **38:** 576–589.

Huang EY, Zhang J, Miska EA, Guenther MG, Kouzarides T, Lazar MA. 2000. Nuclear receptor corepressors partner with class II histone deacetylases in a Sin3-independent repression pathway. *Genes Dev* **14:** 45–54.

Huang W, Ramsey KM, Marcheva B, Bass J. 2011. Circadian rhythms, sleep, and metabolism. *J Clin Invest* **121:** 2133–2141.

Ji H, Jiang H, Ma W, Johnson DS, Myers RM, Wong WH. 2008. An integrated software system for analyzing ChIP–chip and ChIP-seq data. *Nat Biotechnol* **26:** 1293–1300.

Kang HS, Angers M, Beak JY, Wu X, Gimble JM, Wada T, Xie W, Collins JB, Grissom SF, Jetten AM. 2007. Gene expression profiling reveals a regulatory role for RORα and RORγ in phase I and phase II metabolism. *Physiol Genomics* **31:** 281–294.

Kojetin D, Wang Y, Kamenecka TM, Burris TP. 2011. Identification of SR8278, a synthetic antagonist of the nuclear heme receptor REV-ERB. *ACS Chem Biol* **6:** 131–134.

Korach-André M, Parini P, Larsson L, Arner A, Steffensen KR, Gustafsson JA. 2010. Separate and overlapping metabolic functions of LXRα and LXRβ in C57Bl/6 female mice. *Am J Physiol Endocrinol Metab* **298:** E167–E178. doi: 10.1152/ajpendo.00184.2009.

Kuiper GG, Carlsson B, Grandien K, Enmark E, Häggblad J, Nilsson S, Gustafsson JA. 1997. Comparison of the ligand binding specificity and transcript tissue distribution of estrogen receptors α and β. *Endocrinology* **138:** 863–870.

Kumar N, Solt LA, Wang Y, Rogers PM, Bhattacharyya G, Kamenecka TM, Stayrook KR, Crumbley C, Floyd ZE, Gimble JM, et al. 2010. Regulation of adipogenesis by natural and synthetic REV-ERB ligands. *Endocrinology* **151:** 3015–3025.

La Fleur SE. 2003. Daily rhythms in glucose metabolism: Suprachiasmatic nucleus output to peripheral tissue. *J Neuroendocrinol* **15:** 315–322.

Lanza-Jacoby S, Stevenson NR, Kaplan ML. 1986. Circadian changes in serum and liver metabolites and liver lipogenic enzymes in ad libitum- and meal-fed, lean and obese Zucker rats. *J Nutr* **116:** 1798–1809.

Lazar MA. 2003. Nuclear receptor corepressors. *Nucl Recept Signal* **1:** e001. doi: 10.1621/nrs.01001.

Lazar MA, Hodin RA, Darling DS, Chin WW. 1989. A novel member of the thyroid/steroid hormone receptor family is encoded by the opposite strand of the rat c-erbAα transcriptional unit. *Mol Cell Biol* **9:** 1128–1136.

Le Martelot G, Claudel T, Gatfield D, Schaad O, Kornmann B, Sasso GL, Moschetta A, Schibler U. 2009. REV-ERBα participates in circadian SREBP signaling and bile acid homeostasis. *PLoS Biol* **7:** e1000181. doi: 10.1371/journal.pbio.1000181.

Liu AC, Tran HG, Zhang EE, Priest AA, Welsh DK, Kay SA. 2008. Redundant function of REV-ERBα and β and non-essential role for Bmal1 cycling in transcriptional regulation of intracellular circadian rhythms. *PLoS Genet* **4:** e1000023. doi: 10.1371/journal.pgen.1000023.

Lupien M, Meyer CA, Bailey ST, Eeckhoute J, Cook J, Westerling T, Zhang X, Carroll JS, Rhodes DR, Liu XS, et al. 2010. Growth factor stimulation induces a distinct ERα cistrome underlying breast cancer endocrine resistance. *Genes Dev* **24:** 2219–2227.

Miyajima N, Horiuchi R, Shibuya Y, Fukushige S, Matsubara K, Toyoshima K, Yamamoto T. 1989. Two erbA homologs encoding proteins with different T3 binding capacities are transcribed from opposite DNA strands of the same genetic locus. *Cell* **57:** 31–39.

Nielsen R, Grøntved L, Stunnenberg HG, Mandrup S. 2006. Peroxisome proliferator-activated receptor subtype- and cell-type-specific activation of genomic target genes upon adenoviral transgene delivery. *Mol Cell Biol* **26:** 5698–5714.

Panda S, Antoch MP, Miller BH, Su AI, Schook AB, Straume M, Schultz PG, Kay SA, Takahashi JS, Hogenesch JB. 2002. Coordinated transcription of key pathways in the mouse by the circadian clock. *Cell* **109:** 307–320.

Pardee KI, Xu X, Reinking J, Schuetz A, Dong A, Liu S, Zhang R, Tiefenbach J, Lajoie G, Plotnikov AN, et al. 2009. The structural basis of gas-responsive transcription by the human nuclear hormone receptor REV-ERBβ. *PLoS Biol* **7:** e43. doi: 10.1371/journal.pbio.1000043.

Preitner N, Damiola F, Lopez-Molina L, Zakany J, Duboule D, Albrecht U, Schibler U. 2002. The orphan nuclear receptor REV-ERBα controls circadian transcription within the positive limb of the mammalian circadian oscillator. *Cell* **110:** 251–260.

Privalsky ML. 2004. The role of corepressors in transcriptional regulation by nuclear hormone receptors. *Annu Rev Physiol* **66:** 315–360.

Raghuram S, Stayrook KR, Huang P, Rogers PM, Nosie AK, McClure DB, Burris LL, Khorasanizadeh S, Burris TP, Rastinejad F. 2007. Identification of heme as the ligand for the orphan nuclear receptors REV-ERBα and REV-ERBβ. *Nat Struct Mol Biol* **14:** 1207–1213.

Ramakrishnan SN, Lau P, Burke LJ, Muscat GE. 2005. Rev-erbβ regulates the expression of genes involved in lipid absorption in skeletal muscle cells: Evidence for cross-talk between orphan nuclear receptors and myokines. *J Biol Chem* **280:** 8651–8659.

Retnakaran R, Flock G, Giguère V. 1994. Identification of RVR, a novel orphan nuclear receptor that acts as a negative transcriptional regulator. *Mol Endocrinol* **8:** 1234–1244.

Rudic RD, McNamara P, Curtis AM, Boston RC, Panda S, Hogenesch JB, Fitzgerald GA. 2004. BMAL1 and CLOCK, two essential components of the circadian clock, are involved in glucose homeostasis. *PLoS Biol* **2:** e377. doi: 10.1371/journal.pbio.0020377.

Sahar S, Sassone-Corsi P. 2009. Metabolism and cancer: The circadian clock connection. *Nat Rev Cancer* **9:** 886–896.

Shi S, Hida A, McGuinness OP, Wasserman DH, Yamazaki S, Johnson CH. 2010. Circadian clock gene Bmal1 is not essential; functional replacement with its paralog, Bmal2. *Curr Biol* **20:** 316–321.

Sullivan AL, Benner C, Heinz S, Huang W, Xie L, Miano JM, Glass CK. 2011. Serum response factor utilizes distinct promoter- and enhancer-based mechanisms to regulate cytoskeletal gene expression in macrophages. *Mol Cell Biol* **31:** 861–875.

Sun Z, Feng D, Everett LJ, Bugge A, Lazar MA. 2011. Circadian epigenomic remodeling and hepatic lipogenesis: Lessons from HDAC3. *Cold Spring Harb Symp Quant Biol* doi: 10.1101/sqb.2011.76.011494.

Sun Z, Miller R, Patel R, Chen J, Dhir R, Wang H, Zhang D, Graham M, Unterman T, Schulman G, et al. 2012. Hepatic HDAC3 promotes gluconeogenesis by repressing lipid synthesis and sequestration. *Nat Med* (in press).

Takahashi JS, Hong HK, Ko CH, McDearmon EL. 2008. The genetics of mammalian circadian order and disorder: Implications for physiology and disease. *Nat Rev Genet* **9:** 764–775.

van der Horst GT, Muijtjens M, Kobayashi K, Takano R, Kanno S, Takao M, de Wit J, Verkerk A, Eker AP, van Leenen D, et al. 1999. Mammalian Cry1 and Cry2 are essential for maintenance of circadian rhythms. *Nature* **398:** 627–630.

Wang J, Li Y, Zhang M, Liu Z, Wu C, Yuan H, Li YY, Zhao X, Lu H. 2007. A zinc finger HIT domain-containing protein, ZNHIT-1, interacts with orphan nuclear hormone receptor Rev-erbβ and removes Rev-erbβ-induced inhibition of apoCIII transcription. *FEBS J* **274:** 5370–5381.

Wang J, Liu N, Liu Z, Li Y, Song C, Yuan H, Li YY, Zhao X, Lu H. 2008. The orphan nuclear receptor Rev-erbβ recruits Tip60 and HDAC1 to regulate apolipoprotein CIII promoter. *Biochim Biophys Acta* **1783:** 224–236.

Wijnen H, Young MW. 2006. Interplay of circadian clocks and metabolic rhythms. *Annu Rev Genet* **40:** 409–448.

Wong T, Hildebrandt MA, Thrasher SM, Appleton JA, Ahima RS, Wu GD. 2007. Divergent metabolic adaptations to intestinal parasitic nematode infection in mice susceptible or resistant to obesity. *Gastroenterology* **133:** 1979–1988.

Woo EJ, Jeong DG, Lim MY, Jun Kim S, Kim KJ, Yoon SM, Park BC, Ryu SE. 2007. Structural insight into the constitutive repression function of the nuclear receptor Rev-erbβ. *J Mol Biol* **373:** 735–744.

Yin L, Lazar MA. 2005. The orphan nuclear receptor Rev-erbα recruits the N-CoR/histone deacetylase 3 corepressor to regulate the circadian Bmal1 gene. *Mol Endocrinol* **19:** 1452–1459.

Yin L, Wang J, Klein PS, Lazar MA. 2006. Nuclear receptor Rev-erbα is a critical lithium-sensitive component of the circadian clock. *Science* **311:** 1002–1005.

Yin L, Wu N, Curtin JC, Qatanani M, Szwergold NR, Reid RA, Waitt GM, Parks DJ, Pearce KH, Wisely GB, et al. 2007. Rev-erbα, a heme sensor that coordinates metabolic and circadian pathways. *Science* **318:** 1786–1789.

Yin L, Joshi S, Wu N, Tong X, Lazar MA. 2010. E3 ligases Arf-bp1 and Pam mediate lithium-stimulated degradation of the circadian heme receptor Rev-erbα. *Proc Natl Acad Sci* **107:** 11614–11619.

Yu C, Wang F, Kan M, Jin C, Jones RB, Weinstein M, Deng CX, McKeehan WL. 2000. Elevated cholesterol metabolism and bile acid synthesis in mice lacking membrane tyrosine kinase receptor FGFR4. *J Biol Chem* **275:** 15482–15489.

Rev-erbα and Rev-erbβ coordinately protect the circadian clock and normal metabolic function

Anne Bugge, Dan Feng, Logan J. Everett, et al.

Genes Dev. 2012, **26:**
Access the most recent version at doi:10.1101/gad.186858.112